

## A Functional Model for the Cysteinate-Ligated Non-Heme Iron Enzyme Superoxide Reductase (SOR)

Terutaka Kitagawa,<sup>†</sup> Abhishek Dey,<sup>‡</sup> Priscilla Lugo-Mas,<sup>†</sup> Jason B. Benedict,<sup>†</sup> Werner Kaminsky,<sup>†</sup> Edward Solomon,<sup>\*,‡</sup> and Julie A. Kovacs<sup>\*,†</sup>

Department of Chemistry, University of Washington, Seattle, Washington 98195, and Department of Chemistry, Stanford University, Palo Alto, California 94304

Received July 8, 2006; E-mail: kovacs@chem.washington.edu

Superoxide reductases (SORs) are cysteine-ligated non-heme iron enzymes<sup>1</sup> that reduce superoxide ( $O_2^-$ ) to  $H_2O_2$  in anaerobic microbes.<sup>2</sup> The cysteine of SOR is trans to the  $O_2^-$  binding site and is proposed to play an important role in promoting the catalytic reaction. Herein, we report a rare example of a functional metallo-enzyme active site model, that reduces  $O_2^-$  via a trans thiolate-ligated Fe(III)-peroxo intermediate. The trans thiolate is shown to lower the redox potential, change the spin-state, and dramatically weaken the Fe–O bond, favoring  $O_2^-$  reduction and  $H_2O_2$  release.

Superoxide is a toxic byproduct of dioxygen chemistry that has been linked to a number of disease states.<sup>3</sup> The proposed SOR mechanism involves the oxidative addition of  $O_2^-$  to the open site of the square pyramidal  $Fe^{II}N_4^{His}SCys$  active site<sup>2c</sup> to afford a trans  $SCys$ -ligated  $Fe^{III}$ -peroxo intermediate.<sup>2d,e</sup> This intermediate displays an intense S-to-Fe(III) charge-transfer band at  $\sim 600$  ( $\sim 3500$ ) nm, but has yet to be characterized by vibrational spectroscopy. Iron-peroxo species are extremely difficult to characterize since they are thermally unstable and photolabile. Vibrational data have been reported for mutant SOR (E47A) peroxos generated via the addition of  $H_2O_2$ .<sup>2b,f,g</sup> Whether these are identical to the catalytic SOR intermediate remains to be determined. Although a few well-characterized synthetic nitrogen-ligated iron-peroxos have been reported,<sup>4a,c</sup> there is a paucity of thiolate-ligated analogues.<sup>4b</sup> Since a thiolate is likely to influence the correlation between peroxide binding mode, vibrational parameters, and spin state, synthetic thiolate-ligated peroxos are needed to provide benchmark parameters. Prior to the work reported herein, cis thiolate-ligated  $[Fe^{III}(SMe_2N_4(tren))(OOH)]^+$  (**1**)<sup>4b</sup> was the only reported example of a synthetic thiolate-ligated  $Fe^{III}$ -peroxo.

In situ deprotection and deprotonation of the new macrocyclic ligand cyclam-PrS-Ac $\cdot$ 4HCl, afforded  $[Fe^{II}(cyclam-PrS)](BPh_4)$  (**2**) upon the addition of  $FeCl_2$  and  $NaBPh_4$ . Single crystals were grown from pentane/THF at  $-30$  °C. As shown in the ORTEP (Figure 1), the  $Fe^{2+}$  ion of **2** is ligated by three secondary amines, one tertiary amine, and a tethered apical thiolate in a square pyramidal geometry ( $\tau = 0.13$ )<sup>5</sup> resembling that of SOR. A related tertiary amine cyclam complex  $[Fe^{II}(Me_3-cyclam-EtS)]^+$  (**3**) was recently reported<sup>6</sup> that reacts with  $H_2O_2$  to afford an  $Fe(IV)=O$ .<sup>7</sup> Like the SOR active site, **2** is high spin ( $S = 2$ ;  $\mu_{eff} = 5.03 \mu_B$  (MeCN);  $4.91 \mu_B$  (solid)). The Fe–S bond length in **2** (2.286(1) Å) falls in the usual range for synthetic Fe(II)-thiolates,<sup>6,8</sup> but is slightly shorter than that of SOR (Fe–S = 2.4 Å), the cysteine sulfur of which is H-bonded to the protein backbone.<sup>2a,c</sup>

Thiolate-ligated **2** reacts rapidly with  $O_2^{\cdot-}$  (18-crown-6- $K^+$  salt) in  $CH_2Cl_2$  at  $-78$  °C to afford a metastable burgundy intermediate, as soon as a proton donor (MeOH; 82 equiv) is added. This intermediate is high-spin ( $g = 7.72, 5.40, 4.15$ ), and displays an absorp-

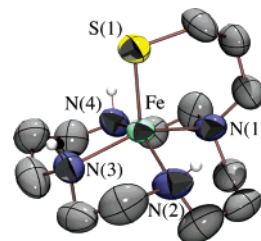


**Figure 1.** ORTEP of  $[Fe^{II}(cyclam-PrS)]^+$  (**2**). Selected bond lengths (Å): Fe–S(1), 2.286(1); Fe–N(1), 2.181(4); Fe–N(2,3,4)<sub>avg</sub>, 2.16(2).

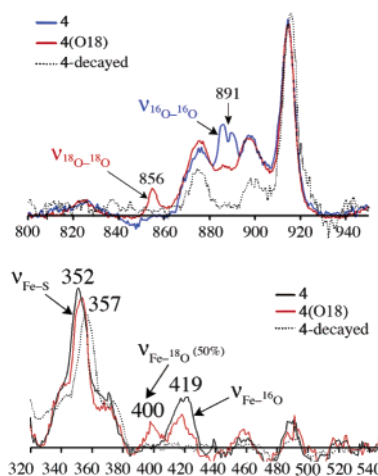


**Figure 2.** rRaman spectra of **4** generated from  $^{16}O_2^-$  (blue),  $^{18}O_2^-$  (red), and “decayed” product (dashed black) (571 nm excitation @ 183 K in THF/MeOH (upper panel); at 77 K in  $CH_2Cl_2$ /THF/MeOH (lower panel).

tion band at  $\lambda_{max} = 530$  (1350) nm. Resonance Raman shows  $\nu_{O-O}$ ,  $\nu_{Fe-O}$ , and  $\nu_{Fe-S}$  stretches at 891 (Fermi doublet), 419, and 352  $cm^{-1}$ , respectively (Figure 2).  $K^{18}O_2$  (50% enriched; ICON) causes the  $\nu_{O-O}$  and  $\nu_{Fe-O}$  to shift to 856 and 400  $cm^{-1}$ , respectively, and addition of  $D^+$  (i.e., MeOD) causes the Fermi doublet to collapse. These data are consistent with the formation of an Fe–hydroperoxo species,  $[Fe^{III}(cyclam-PrS)(OOH)]^+$  (**4**), via the proton-dependent oxidative addition of superoxide to **2**. No reaction occurs in the absence of a proton donor, and  $O_2^-$  does not convert to  $H_2O_2$  in the absence of **2**, under the conditions examined ( $-78$  °C, 82 equiv MeOH). Intermediate **4** represents the first example of a synthetic trans thiolate-ligated  $Fe^{III}$ -peroxo SOR intermediate analogue, the characterization of which provides important benchmark parameters.

The  $\nu_{Fe-O}$  stretch of **4** is significantly lower than all other reported synthetic iron peroxides (range: 450–639  $cm^{-1}$ )<sup>4a</sup> but compares well with that of the only reported SOR peroxo (438  $cm^{-1}$ ).<sup>2a,e</sup> The  $\nu_{O-O}$  stretch (891  $cm^{-1}$ ) is unusually high (reported range: 820–860  $cm^{-1}$ ).<sup>4a</sup> The DFT optimized structure of **4** minimizes with Fe–S and Fe–O distances of 2.36 and 1.95 Å,

<sup>†</sup> University of Washington.

<sup>‡</sup> Stanford University.

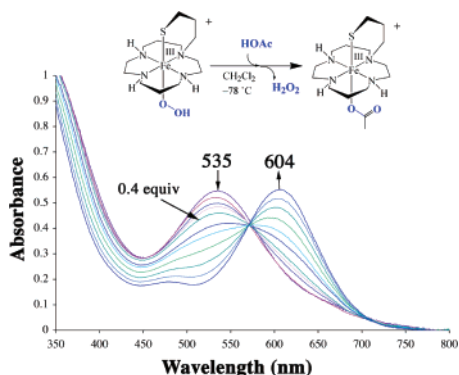


**Figure 3.** Conversion of peroxo-bound **4** (0.5 mM in  $\text{CH}_2\text{Cl}_2$ ) to acetate-bound  $[\text{Fe}^{\text{III}}(\text{cyclam-PrS})(\text{OAc})]^+$  (**5**) via the addition of HOAc (0.1 equiv aliquots every 2 min) at  $-78^\circ\text{C}$ .

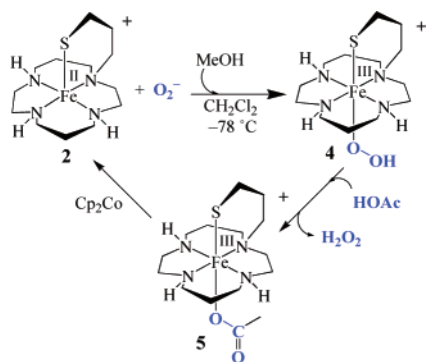


**Figure 4.** The catalytic cycle involving  $[\text{Fe}^{\text{II}}(\text{cyclam-PrS})]^+$  (**2**) induced superoxide ( $\text{O}_2^-$ ) reduction

respectively, and a protonated peroxo O–O distance of 1.44 Å. This Fe–O (peroxo) distance is significantly longer than the few reported Fe–( $\eta^1$ -OOH) structures (1.76–1.86 Å)<sup>4a,b</sup> reflecting the trans influence of the thiolate sulfur. The calculated  $\nu_{\text{Fe-S}}$  (345  $\text{cm}^{-1}$ ),  $\nu_{\text{Fe-O}}$  (400  $\text{cm}^{-1}$ ), and  $\nu_{\text{O-O}}$  (933  $\text{cm}^{-1}$ ) stretches are in reasonable agreement with the experimental data. When the thiolate is replaced with an amine or alkoxide, trans to the peroxo,<sup>9</sup> then the calculated  $\nu_{\text{Fe-O}}$  (495 and 420  $\text{cm}^{-1}$ , respectively) is considerably higher. These vibrational data, along with the calculated force constant ( $k_{\text{Fe-O}} = 1.20 \text{ mdyne/cm}^2$  for **4** vs reported range = 2.2–2.1  $\text{mdyne/cm}^2$ ),<sup>4a</sup> indicate that the Fe–O (peroxide) bond is significantly weakened upon the introduction of a trans thiolate into the coordination sphere.

Addition of HOAc to metastable **4** at  $-78^\circ\text{C}$  releases  $\text{H}_2\text{O}_2$  (as detected using an amplex red assay), and cleanly affords a new aqua blue species  $\lambda_{\text{max}} = 604$  (1350 nm) (Figure 3). When this reaction is monitored by EPR, the high-spin signal associated with **4** is replaced with a new low-spin signal at  $g = 2.37, 2.30, 1.89$ . The  $\nu_{\text{O-O}}$  and  $\nu_{\text{Fe-O}}$  stretches disappear in the rRaman spectrum, and new stretches are observed at 339, 409, and 421  $\text{cm}^{-1}$ . Although this aqua blue species proved too unstable to isolate, it was unambiguously identified by ESI-mass spectrometry as acetate-bound  $[\text{Fe}^{\text{III}}(\text{cyclam-PrS})(\text{OAc})]^+$  (**5**), a model for Glu-bound SOR.

Addition of a sacrificial reductant ( $\text{Cp}_2\text{Co}$ ) to **5** at low temperatures ( $-78^\circ\text{C}$ ) regenerates **2**, which then reacts with a second equivalent of  $\text{O}_2^-$  to re-afford peroxo **4**. Addition of a second equivalent of HOAc releases  $\text{H}_2\text{O}_2$  (Figure 4), thereby mimicking the proposed SOR catalytic cycle involving glutamic acid,<sup>2d,e,i</sup> and demonstrating that reduction of  $\text{O}_2^-$  by **2** is catalytic. Thus far, five turnovers have been achieved.

The thiolate ligand and its trans positioning relative to the substrate appear to contribute significantly to the function of our

biomimetic catalyst. First, the pendant thiolate arm of **2** causes the redox potential to shift anodically by +480 mV relative to  $[\text{Fe}^{\text{II}}(\text{cyclam})(\text{MeCN})_2]$  (from +700 to +220 mV vs SCE), making it better suited to promote superoxide reduction. Second, the trans thiolate changes the spin state from  $S = 1/2^{\text{ab}}$  to  $S = 5/2$ : the majority of nitrogen-ligated Fe(III)-OOH's are  $S = 1/2$ ,<sup>4a</sup> as is cis thiolate-ligated **1**.<sup>4b</sup> Third, the thiolate dramatically shifts the  $\nu_{\text{Fe-O}}$  stretch and decreases the  $k_{\text{Fe-O}}$  force constant well-below all other reported iron peroxides.<sup>4a</sup> Peroxo **4** partially converts to methoxide-bound  $[\text{Fe}^{\text{III}}(\text{cyclam-PrS})(\text{OMe})]^+$  (**6**;  $g = 2.34, 2.26, 1.95$ ;  $\nu_{\text{Fe-S}} = 357 \text{ cm}^{-1}$ ) within minutes at  $-78^\circ\text{C}$ , whereas cis-ligated peroxo **1** takes hours ( $t_{1/2} = 63.9 \text{ h}$ ) to convert to  $[\text{Fe}^{\text{III}}(\text{S}^{\text{Me}_2\text{N}_4}(\text{tren}))(\text{OMe})]^+$  under the same conditions. Methoxide-bound **6** was identified via its independent synthesis involving  $\text{Cp}_2\text{Fe}^+$  oxidation of **2** in MeOH, in the presence of  $^i\text{Pr}_2\text{EtN}$ .

In conclusion, the data described herein indicate that like the enzyme, SOR intermediate-analogue **4** is better suited to promote Fe–O, as opposed to O–O, bond cleavage. This is in contrast to P450 and its analogue **3**. Kinetics studies and studies aimed at determining the  $\text{p}K_{\text{a}}$  of the proximal and distal peroxo oxygens of **4** are currently underway.

**Acknowledgment.** This research was supported by NIH Grant GM45881 (J.A.K.), Grant GM40392 (E.I.S.), and Fellowship F31 GM73583 (P.L.-M.).

**Supporting Information Available:** Detailed ligand syntheses and description of UV/vis monitored catalytic turnover,  $^1\text{H}$  NMR, ESI mass spectrometry (ligand, **5**), EPR,  $1/\chi$  vs  $T$  plot and CV of **2**, UV/vis of **4**, Amplex red assay, and X-ray tables. This material is available free of charge via the Internet at <http://pubs.acs.org>.

## References

- (1) Kovacs, J. A. *Chem. Rev.* **2004**, *104*, 825–848.
- (2) (a) Kurtz, D. M., Jr. *Acc. Chem. Res.* **2004**, *37*, 902–908. (b) Mathé, C.; Niviere, V.; Houée-Levin, C.; Mattioli, T. A. *Biophys. Chem.* **2006**, *119*, 38–48. (c) Yeh, A. P.; Hu, Y.; Jenney, F. E., Jr.; Adams, M. W. W.; Rees, D. C. *Biochemistry* **2000**, *39*, 2499–2508. (d) Emerson, J. P.; Coulter, E. D.; Cabelli, D. E.; Phillips, R. S.; Kurtz, D. M., Jr. *Biochemistry* **2002**, *41*, 4348–4357. (e) Niviere, V.; Asso, M.; Weill, C. O.; Lombard, M.; Guigliarelli, B.; Favaudon, V.; Houée-Levin, C. *Biochemistry* **2004**, *43*, 808–818. (f) Mathe, C.; Mattioli, T. A.; Horner, O.; Lombard, M.; Latour, J.-M.; Fontecave, M.; Niviere, V. *J. Am. Chem. Soc.* **2002**, *124*, 4966–4967. (g) Horner, O.; Mousca, J.-M.; Oddou, J.-L.; Jeandey, C.; Niviere, V.; Mattioli, T. A.; Mathe, C.; Fontecave, M.; Maldivi, P.; Bonville, P.; Halfen, J. A.; Latour, J.-M. *Biochemistry* **2004**, *43*, 8815–8825. (h) Mathé, C.; Niviere, V.; Mattioli, T. A. *J. Am. Chem. Soc.* **2005**, *127*, 16436–16441. (i) Clay, M. D.; Jenney, F. E., Jr.; Hagedoorn, P. L.; George, G. N.; Adams, M. W. W.; Johnson, M. K. *J. Am. Chem. Soc.* **2002**, *124*, 788–805. (j) Jovanovic, T.; Axcenso, C.; Hazlett, K. R. O.; Sikkink, R.; Krebs, C.; Litwiller, R.; Benson, L. M.; Moura, I.; Moura, J. J. G.; Radolf, J. D.; Huynh, B. H.; Naylor, S.; Rusnak, F. *J. Biol. Chem.* **2000**, *275*, 28439–28448.
- (3) (a) Gogun, Y.; Sakurada, S.; Kimura, Y.; Nagumo, M. *J. Clin. Biochem. Nutr.* **1990**, *8*, 85–92. (b) Kocaturk, P. A.; Akbostanci, M. C.; Tan, F.; Kavas, G. O. *Pathophysiology* **2000**, *7*, 63–67. (c) Ihara, Y.; Chuda, M.; Kuroda, S.; Hayabara, T. *J. Neurol. Sci.* **1999**, *170*, 90–95. (d) De Leo, M. E.; Borrello, S.; Passantino, M.; Palazzotti, B.; Mordente, A.; Daneile, A.; Filippini, V.; Galeotti, T.; Masullo, C. *Neurosci. Lett.* **1998**, *250*, 173–176.
- (4) (a) Roelfes, G.; Vrajmasu, V.; Chen, K.; Ho, R. Y. N.; Rohde, J.-U.; Zondervan, C.; la Crois, R. M.; Schudde, E.P.; Lutz, M.; Spek, A. L.; Hage, R.; Feringa, B. L.; MuncK, E.; Que, L., Jr. *Inorg. Chem.* **2003**, *42*, 2639–2653. (b) Shearer, J.; Scarrow, R. C.; Kovacs, J. A. *J. Am. Chem. Soc.* **2002**, *124*, 11709–11717. (c) Ballard, V.; Bance, F.; Anxolabehere-Mallart, E.; Ghiladi, M.; Mattioli, T. A.; Philouze, C.; Blondin, G.; Girerd, J.-J. *Inorg. Chem.* **2003**, *42*, 2470–2477.
- (5) Addison, A. W.; Rao, T. N.; Reedijk, J. *J. Chem. Soc., Dalton Trans.* **1984**, 1349.
- (6) Fiedler, A. T.; Halfen, H. L.; Halfen, J. A.; Brunold, T. C. *J. Am. Chem. Soc.* **2005**, *127*, 1675–1689.
- (7) Bukowski, M. R.; Koehntop, K. D.; Stubna, A.; Bominaar, E. L.; Halfen, J. A.; Münck, E.; Nam, W.; Que, L., Jr. *Science* **2005**, *310*, 1000–1002.
- (8) (a) Shearer, J.; Nehring, J.; Kaminsky, W.; Kovacs, J. A. *Inorg. Chem.* **2001**, *40*, 5483–5484. (b) Noveron, J. C.; Olmstead, M. M.; Mascharak, P. K. *J. Am. Chem. Soc.* **2001**, *123*, 3247–3259.
- (9) Lehnert, N.; Ho, R. Y. N.; Que, L. Jr.; Solomon, E. I. *J. Am. Chem. Soc.* **2001**, *123*, 12802–12816.

JA064870D